analytical chemistry

Article

pubs.acs.org/ac

Evaporation-Driven Bioassays in Suspended Droplets

Ruth Hernandez-Perez,[†] Z. Hugh Fan,[‡] and Jose L. Garcia-Cordero*[,†]

[†]Unidad Monterrey, Centro de Investigacion y de Estudios Avanzados del Instituto Politecnico Nacional, Via del Conocimiento 201, Parque PIIT, Apodaca, Nuevo León CP 66628, Mexico

[‡]Department of Mechanical and Aerospace Engineering, University of Florida, P.O. Box 116250, Gainesville, Florida 32611, United States

Supporting Information

ABSTRACT: The microtiter plate has been an essential tool for diagnostics, high-throughput screening, and biological assays. We present an alternative platform to perform bioassays in a microplate format that exploits evaporation to drive assay reactions. Our method consists of droplets suspended on plastic pillars; reactions occur in these droplets instead of the wells. The pillars are fabricated by milling, and the rough surface created by this fabrication method pins the droplet to a constant contact line during the assay and also acts as a hydrophobic surface. Upon evaporation, natural convection arising from Marangoni currents mixes solutions in the droplet, which speeds up assay reactions, decreases assay times, and increases limits of detection. As a proof of concept we implemented two colorimetric assays to detect glucose and proteins in only 1.5 μL, without any external devices for mixing and with a digital microscope as a readout mechanism. Our platform is an ideal alternative to the microtiter plate, works with different volumes, is compatible with commercially available reagent dispensers and plate-readers, and could have broad applications in diagnostics and high-throughput screening.

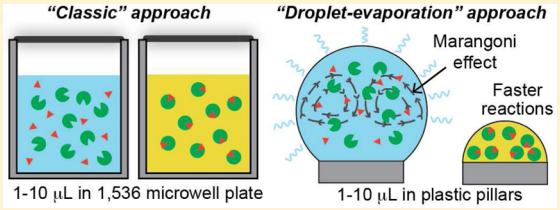

The microtiter plate, or microplate, has been one of the main workforce tools in standard clinical analysis, in biological laboratories, and in the pharmaceutical industry.[1] It is essentially a flat plate embedded with dozens of wells that serve as reaction vessels. A whole industry has been developed around these plates and their supporting peripherals which include automatic plate readers, pipettes, and automatic liquid handling units.[2] To accommodate smaller sample volumes, the microtiter plate has evolved from the original 96 wells per plate with a typical working volume capacity of 50−200 μL to higher density microplates in the same footprint: 384-well (5−100 μL), 1536-well (2.5−10 μL), and more recently 3456-well plates (1−2 μL).[3] Lower volumes translate into increased sample throughput, reagent cost reduction, and faster analysis times, all within the same plate footprint—thus the push to translate assays to higher density plates especially for precious samples and expensive reagents.[4]

Most assays carried out in 96- and 384-well plates consist of six basic actions: (i) pipetting reagents or samples, (ii), adding assay reagents, (iii) mixing by either pipetting up and down or shaking, (iv) incubation, (v) washing, and (vi) signal readout. While successful adaptation of assays from the 96- and 384-well plate format to a 1536-well microplate[3] has been reported, transferring it to lower volumes, and thus higher densities plates, remains difficult, even for 1536-well plates. Indeed, the challenge remains on the microliquid handling techniques rather than the measurement methods.[5] One concomitant issue working at volumes <5 μL is mixing. For different reagents amounts, efficient mixing within a well is a bottleneck in microplates.[6] Strategies such as vortexing, magnetic stirring, ultrasound, and layering the solution with a solvent have been employed for rapid mixing in plate wells.[6,7] But each of them has its own shortcomings: mechanical agitation is inhibited due to adhesive and cohesive forces, vortexers causes foaming, magnetic stir elements interfere with optical measurements, ultrasound mixing requires a transducer inside the medium or in close contact to the well, and solvent addition can interfere with the assay.[7] In addition, most of these strategies increase the cost of instrumentation. Therefore, swift mixing strategies which avoid external devices are in much need.

Another issue working with low volumes (<5 μL) is evaporation, which is usually avoided with humidity control or by covering the plate with a plastic film or an aluminum foil. For even lower volumes (0.3 μL) agarose can be used to control evaporation.[2] For volumes less than 1 μL the shape of the wells has to be redesigned and molded from special materials,[2] which translate into higher fabrication costs. In addition, the increase in surface-to-volume ratio can affect stability and adsorption of reagents to the walls.[3] Therefore, alternative formats to the microtiter plate formats are desired which respect the footprint standards, are compatible with their supporting peripherals, are easy to fabricate, and reduce evaporation while maintaining assay performance, stability, and accuracy.

In this paper we introduce a new method to perform bioassays on suspended droplets. These droplets reside on the

Received: April 26, 2016
Accepted: June 22, 2016
Published: June 22, 2016

DOI: 10.1021/acs.analchem.6b01657
Anal. Chem. 2016, 88, 7312−7317

surface of a plastic pillar-like structure fabricated by milling (Figure 1). Instead of performing an assay within an enclosed

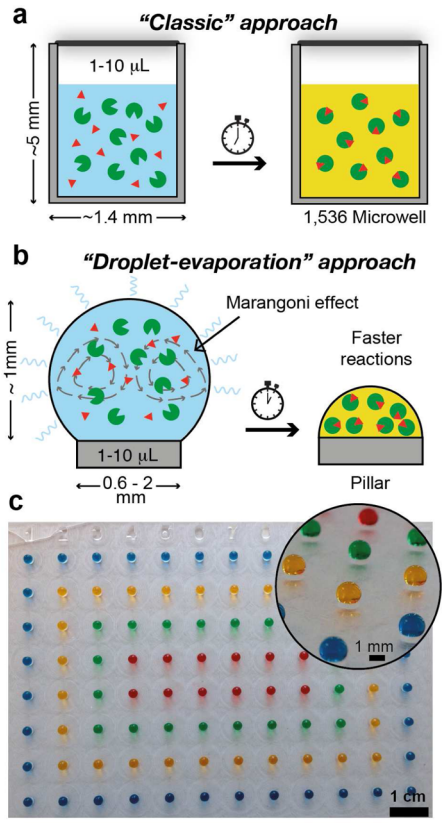

Figure 1. (a) Comparison of assays carried out on wells in a 384- or a 1536-well microtiter plate and (b) in our pillar platform. Assays in microwells are sealed so that they will not evaporate, whereas we exploit natural evaporation to reduce assay time and increase sensitivity. (c) Close-up and photograph of a 96-pillar array with an equal amount of droplets. The pillar plate is the same size as a 96 microtiter plate.

vessel we propose to carry them out in the open atmosphere. We exploit evaporation as a natural mixing strategy, which not only decreases assay time but also increases its dynamic detection range, compared to a droplet lying on a flat surface. We show that these pillars are easily fabricated with a milling machine, and we demonstrate applications of this platform to the colorimetric detection of glucose and proteins, although other assays should be feasible to implement in this format.

EXPERIMENTAL SECTION

Fabrication of Pillars. Devices were designed in Dr. Engrave (Roland DG, Germany) and fabricated on a 1.5 mm thick poly(methyl methacrylate) (PMMA) sheet using a high-precision milling machine (MDX-40A, Roland DG, Germany). Pillars were engraved with a 1 mm tungsten carbide drill bit at 6000 rpm. Unless otherwise indicated, pillars had a width of 800 μm and height of 1 mm. Pillars were blow-dried with an N_2 gun, covered with a plastic film, and stored in a closed container at room temperature before usage.

Humidity-Controlled Chamber. Experiments were carried out inside a custom-built humidity chamber. The chamber is made of 1 in. thick acrylic covered with layer of white paper and a polarized silver film to reduce light reflections and facilitate image analysis. Its dimensions are 30 cm × 30 cm × 50 cm. A 500 lm white light source (902-838, Ecosmart, U.S.A.) was placed inside the chamber and on top of the pillars. The chamber also contained a 20 kHz ultrasonic humidifier (AIR-200, Steren, Mexico), a container of silica gel, and a cooling fan (TFD-8025M12S, Titan, Taiwan).

Electronic Control. An on−off control was implemented in an Arduino UNO board to maintain a constant humidity for the duration of the experiments. The humidifier was controlled with a relay board. Humidity inside the chamber was monitored with a humidity sensor (FSH75, Sensirion, Switzerland). A graphical user interface was designed in LabView to monitor in real time the variations of humidity and temperature in the chamber.

Image Acquisition and Analysis. Two USB digital microscopes, both with a magnification of 300× monitored the evaporation of droplets on the pillars. One microscope (AM2111, Dino Lite, Taiwan) viewed the top of the pillar, while the other (Microcapture Pro 5MP, Celestron, U.S.A.) faced it sideways. Images were captured automatically every minute and saved as bmp files. The evolution of the droplet's contact angle and height was analyzed using the low bond axisymmetric drop shape analysis (LBADSA) plug-in from ImageJ; a script in Matlab calculated the volume with this data. The change in color on the pillar was evaluated with a custom-made algorithm in Matlab in which the user manually adjusts a circle to the size of the pillar. The algorithm converts the original images to the CMYK (cyan, magenta, yellow, and black) color space system and averages the intensity of the pixels from the circle using only the black channel data.

Solution Preparation. Unless otherwise indicated all reagents were purchased from Sigma-Aldrich (U.S.A.). Samples of glucose (G3660) were prepared at concentrations of clinically relevant ranges, from 2.5 to 50 mM. A mixture of an enzyme solution of 15 U/mL of horseradish peroxide (HRP)/gluxcose oxidase (GOx) was prepared by dissolving a capsule containing 500 units of GOx (*Aspergillus niger*), 100 units of HRP (pupurogallin units), and phosphate buffer in 39.2 mL of deionized water. This solution was stored in the dark at −20 °C. A solution of HRP/GOx diluted 10:1 in a chromogen (potassium iodide, P2963) was made before performing an experiment and kept at 4 °C.

Glucose Assay. Experiments were carried out at room temperature. In general, the conditions inside the chamber were kept below 50% humidity and at a temperature of 24 °C. With the chamber open, a metal tip was fitted to a 10 μL pipet tip and used to deposit 2 μL of the HRP/GOx/chromogen onto the surface of the pillar. This solution was allowed to evaporate until the volume reached 500 nL followed by addition of 1 μL of glucose. We monitored the height of the drops to confirm that we deposited the same volume every time. The chamber was closed and the fan activated to induce evaporation; the evolution of the drop was monitored for the duration of the experiment, ~25 min, or until the reaction was completed.

Protein Assay. A solution of 125 mM citrate buffer at pH 1.8 was prepared in 92% water and 8% ethanol by volume. This solution was mixed in a 10:1 ratio in a solution of 9 mM tetrabromophenol blue (TBPB) in 95% ethanol and 5% water. Solutions of bovine serum albumin (BSA) at concentrations ranging from 10 to 60 μM were prepared. A drop of 0.8 μL was placed on a pillar and allowed to evaporate completely in the dark; then, 0.8 μL of the protein sample was placed over this solution and allowed to react. The use of air flow was not

DOI: 10.1021/acs.analchem.6b01657
Anal. Chem. 2016, 88, 7312−7317

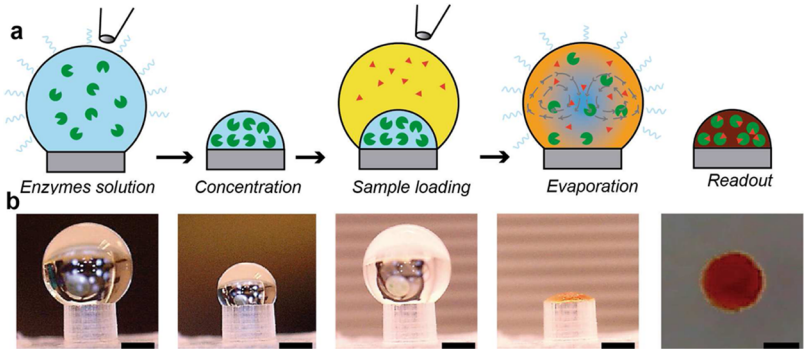

Figure 2. (a) Schematic diagram of a colorimetric assay and (b) photos of the actual assay in a pillar. The assay includes five basic steps: (i) spotting of enzymes solution, (ii) concentration of this solution after evaporation, (iii) spotting of sample, (iv) mixing by the Marangoni effect, a byproduct of evaporation, and (v) signal readout with a digital camera or a smartphone. Scale bar: 500 μm.

necessary in this assay because this solution contains ethanol which evaporates faster than water and the color disappears upon full evaporation.

RESULTS AND DISCUSSION

Our pillar platform effectively consists of a cylinder structure carved out of acrylic, although it is possible to use other plastic materials. Assays occur over the surface of this cylinder, Figure 1, compared to how reactions occur in a microwell where the top is generally sealed with a film. In addition, the bottom length of a square well is 1.4 mm while the diameter of our pillars can be as small as 0.6 mm to accommodate 1 μL volume samples. The roughness created on the edge of the pillar by the fabrication process (micromilling) allows the pinning of any solution to the surface of the pillar and prevents wetting of the pillar walls; thus, the pillar essentially acts as a superhydrophobic surface with contact angles greater than 140° for water. We were able to place up to 10 μL volumes on a 1.8 mm diameter pillar without any spills. While other methods exist to create hydrophobic and superhydrophobic surfaces using lengthy micro- and nanofabrication techniques[8−10] or chemical methods,[9] our technique is simpler, faster, and less expensive, and permits the user to define the precise location and the number of pillars in a plate. For example, we fabricated a microtiter plate with 96 pillars in fewer than 10 min, Figure 1c.

Compared to microtiter plates, our pillars benefit from evaporation first, by increasing the concentration through a volume reduction, and second, by convective mixing arising from Marangoni flow currents.[11] The hydrodynamics of an evaporating sessile droplet have been extensively studied.[12−14] The nonuniform evaporation rate across the surface of the droplet causes radial flow inside it. Colloids (if present) in a solution are carried by these radial currents to the contact line (i.e., the air−water−substrate interface), which pins the droplet to the contact line preventing it from receding during evaporation, thus leaving a distinctive radial pattern known as the coffee ring effect.[15,16] The higher rate of evaporation along the contact line produces these flow patterns (or capillary flow), also known as primary radial flow.[17] The coffee ring effect has been exploited to perform immunoassays and to separate particles by size.[12,18−20]

In contrast to a flat surface, the pillar pins the droplet to its perimeter maintaining a constant contact line throughout evaporation, but also increases the contact angle for most of the evaporation process and deters the appearance of the coffee ring effect from the onset of the reaction. Secondary radial flow, also known as the Marangoni effect, is produced by differences in surface tension on the free liquid surface of the droplet.[21,22] These differences in surface tension are either produced by temperature gradients or by solute concentration along the droplet surface.[21,22] Marangoni stresses induce secondary flows that recirculates the liquid to the center of the drop as it evaporates.[12] We observed Marangoni-induced flows on evaporating droplets using fluorescent microparticles (Supporting Information Video 1). Chaotic advection is also observed in a glucose colorimetric assay (Supporting Information Video 2). However, further characterization of these secondary flows is needed; this could be achieved using particle image velocimetry or optical coherence tomography.[12]

A typical flowchart for a colorimetric assay using our pillar platform and actual photographs of this process are shown in Figure 2. A drop containing the enzyme is placed on top of the pillar and allowed to evaporate. This is followed by depositing the sample over this preconcentrated solution. Upon evaporation, both solutions start to mix by the Marangoni effect and a color starts developing as both enzyme and substrate react. Note that the concentration step as a result of evaporation is very beneficial for those real-world samples with low abundance. Once completely evaporated a picture is taken in which the color intensity is proportional to the analyte concentration.

We wondered how a reaction would develop in a drop suspended on a pillar in a high- and low-humidity environments, compared to a flat surface. Figure 3 follows a glucose colorimetric assay under these three different scenarios. We monitored a glucose solution of 10 mM (average physiological value) for 20 min taking photographs from the top and sideways. As expected, a 1.5 μL drop placed on a 800 μm pillar inside a chamber with a high humidity (>90%) did not evaporate, nor did it show a change in color after even 1 h (Figure 3a), further corroborating that diffusion is not enough to start the reaction and that, indeed, secondary current flows are necessary to mix the solution and the enzymes. A drop placed in an acrylic sheet exhibits a low contact angle (60°) and occupies a diameter of 2.3 mm, more than twice the diameter and 8 times the surface area of the pillar (Figure 3c). As the droplet evaporates there is a change in color but also the appearance of the coffee ring effect. In contrast, a drop placed over a pillar in a low-humidity environment (40%) starts reacting with the substrate, giving rise to a dim yellow color (Figure 3b). The initial contact angle of the droplet was 150°, compared to 60° on a flat surface; it is important to highlight

DOI: 10.1021/acs.analchem.6b01657
Anal. Chem. 2016, 88, 7312−7317

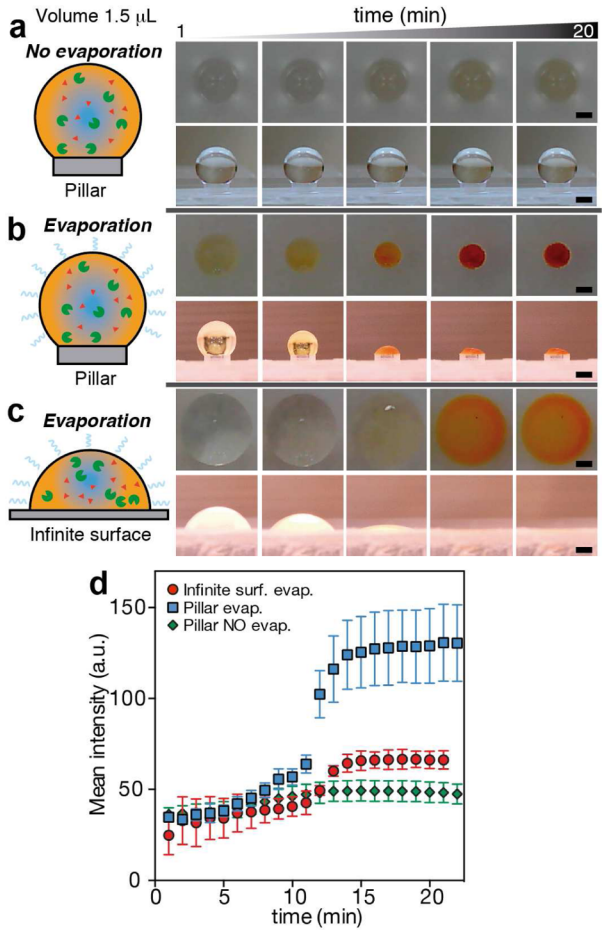

Figure 3. Behavior of a colorimetric assay performed on a 1.5 μL droplet under different conditions: (a) on a 800 μm diameter pillar with no evaporation, (b) on a pillar with evaporation, and (c) on a flat surface with evaporation. Series of images show the top and side view of the droplet over a 20 min period. (d) Colorimetric data of a 10 mM glucose solution for these three different conditions. Error bars represent the standard deviation for three experiments. Scale bar: 500 μm.

this, as higher contact angles correspond to higher Marangoni number, which in turn are proportional to the velocity currents in the droplet (or strength of the recirculation) and, therefore, to a better convective mixing.[11,22] After 15 min the intensity from the pillar is twice the value than the flat surface because iodine particles are concentrated in a smaller area. Surprisingly, the rate of evaporation of drops on the pillar and the flat surface is about the same. In addition, the increase in viscosity as the drop evaporates eliminates the appearance of the coffee ring, giving a more uniform color compared to the droplet on an extended surface, which also facilitates the measurements.

Next, we studied the kinetics of a glucose colorimetric assay in our pillar platform. Although blood glucose levels in humans fluctuate throughout the day, fasting normal values oscillate between 70−100 mg/dL (3.8−5.5 mM); fasting values of 100−125 mg/dL (5.5−7 mM) could indicate a prediabetes alteration, and values higher than 200 mg/dL (11.1 mM) are symptomatic of diabetes. We observed the protocol shown in Figure 2 and prepared glucose solutions ranging from 0 to 50 mM. We first spotted a solution of 1 μL of GOx, HRP, and potassium iodide, and allowed the mixture to evaporate to a volume of 500 nL. Next, we loaded 1 μL of the sample over that solution.

Data and error bars from five independent measurements performed on different days, using one pillar per assay, are shown in Figure 4a. Signals in the assay response were

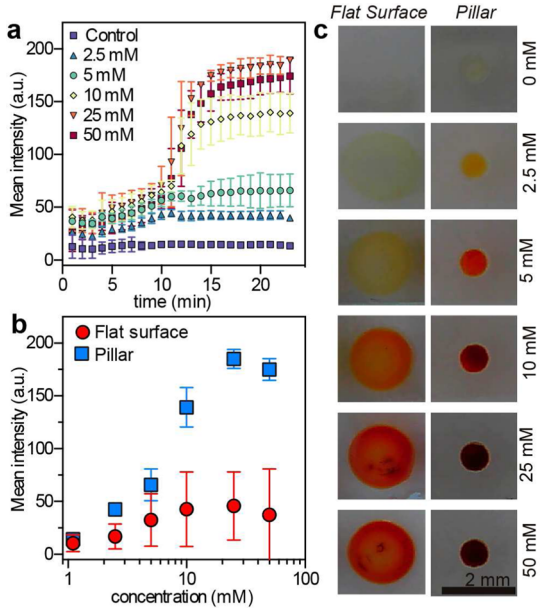

Figure 4. (a) Characterization of glucose enzymatic assay for a glucose concentration range of 0−50 mM performed in a 1.5 μL droplet on a 800 μm pillar. The initial GOx concentration was 6.25 nM. Error bars represent the standard deviation for five experiments. (b) End-point values are compared to the same reaction on a flat surface. (c) Top-view photographs of the reaction after 20 min for both, a flat surface (left) and a pillar (right).

quantitated by measuring a circular region of interest (the size of the pillar) on the image and the original format converted to the CMYK color space, using only the black channel value for the analysis. We evaluated different color spaces but found that for this particular assay the black channel from the CMYK space gave the best results. From Figure 4a, it can also be observed that the end-point color intensity and the reaction velocity correlate with glucose concentration. The kinetics of a GOx reaction follow the model described by the Michaelis−Menten equation:[23]

$$\upsilon = (V_{max}[\mathrm{Glu}])/(K_M + [\mathrm{Glu}]) \quad (1)$$

where υ refers to the initial rate of transport at substrate concentration [Glu], V_{max} is the maximum initial rate of transport at very high substrate concentration, K_M is the Michaelis−Menten constant, and [Glu] denotes the glucose concentration. To determine K_M and V_{max}, υ can be obtained from analyzing the kinetics of different substrate concentrations.[23,24] For a GOx reaction in steady-state conditions these plots resemble an exponential curve, as has already been observed in free solution and in micro- and nanofluidic channels.[23,24] However, as shown in Figure 4a, the curves we obtained resemble a sigmoidal line in which the reaction occurs very slowly for the first 10 min (enzyme and substrate not mixed) and then ramps up (mixing occurs, steady-state conditions). We attribute this effect to the dynamics of the Marangoni effect, as well as to an increase in substrate concentration as the droplet evaporates. Although a new model

DOI: 10.1021/acs.analchem.6b01657
Anal. Chem. 2016, 88, 7312−7317

must be worked out that takes into account these variables, measuring the reaction kinetics of any reaction can still provide valuable information, such as the enzyme affinity for a substrate. Yet, the end-point values are proportional to the glucose concentration.

The same experiment was carried out on a flat surface and compared to that in the pillar. Figure 4b shows a significant increase in sensitivity when a pillar is used; the color mean intensity plateaus at 25 mM compared to 5 mM on a flat surface. It also shows a linear range from 0 to 15 mM for the pillar, with a limit of detection (LOD) of 2.5 mM; for comparison, commercial dipsticks have a LOD of 5 mM.[25] In addition, the error bars for the drop on a flat surface are significantly greater than for the pillar; this is expected as the coffee ring effect produces a brighter color on the edges of the drop (Figure 4c). A similar problem occurs with paper-based microfluidics where the color distribution is more dispersed and uneven. Only 15 min are required for the color to fully develop (Figure 4a); in contrast, for a microfluidic-based paper device it takes at least 30 min.[26]

We also applied the use of the pillar to the study of a protein colorimetric assay, Figure 5. The solutions and reaction

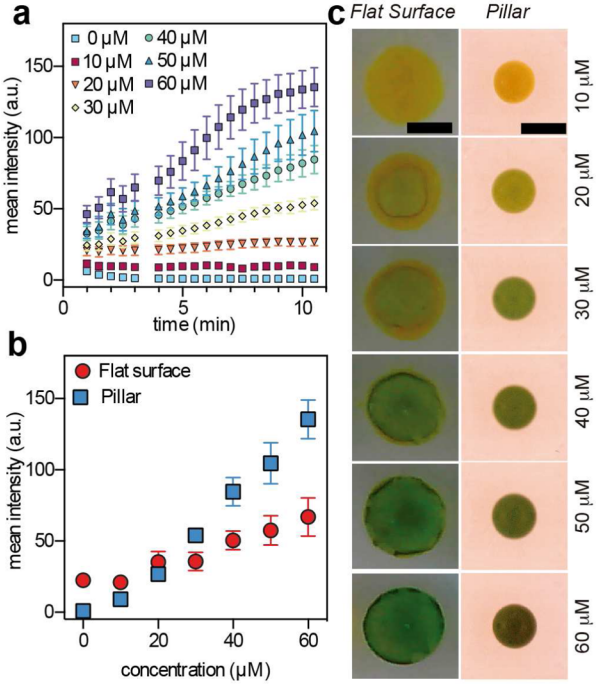

Figure 5. (a) Characterization of protein colorimetric assay for a concentration range of 0−60 μM performed in a 1.5 μL droplet on a 800 μm pillar. (b) End-point values are compared to the same reaction on a flat surface. (c) Top-view photographs of the reaction after 10 min for both, a flat surface (left) and a pillar (right). Scale bar is 1 mm.

mechanism are different from the glucose assay. We used a lower volume of reagents as the presence of ethanol reduces the contact angle and increases the evaporation rate. We spotted a mixture of the citrate buffer solution and TBPB over the pillar and let it evaporate completely. Next, we pipetted 800 nL sample volumes with protein concentrations in relevant clinical ranges (0−60 μM). The solutions start mixing almost instantly producing a change in color that evolves from yellow to green for low and high concentrations, respectively. Indeed, the reaction occurs faster than the glucose assay, in which almost immediately (from minute 1) a difference can be observed between the concentrations. Slower reactions could be possible by decreasing the concentration of reagents. We monitored this reaction every minute as shown in Figure 5a. The range for detecting protein is linear from 0 to 60 μM, while for a flat surface the lowest detectable concentration is 20 μM, Figure 5b. Photographs of both experiments are show in Figure 5c in which is evident the formation of the coffee ring on the flat surface compared to the more homogeneous color for the pillar assay. This is more striking at concentrations below 40 μM where there is an evident difference in color at the edge (yellow) compared to the center (green) of the droplet, while on the pillar the color is more homogeneous.

CONCLUSIONS

The majority of the analytical applications of evaporating droplets have been to preconcentrate analytes into a small area, whether DNA,[8,27,28] protein,[9,10,29,30] heavy metal ions,[31] or nanoparticles.[32] Yet none of these methods include a streamlined protocol to perform bioassays exploiting secondary effects of evaporation, such as the Marangoni effect. Another advantage of our platform is that devices are fabricated with a regular milling machine, which allows the production of pillars on specific locations in short times. Solutions are pinned to the edge of the pillars because of the roughness produced during the fabrication process, thus avoiding common methods to create superhydrophobic surfaces that rely on micro- and nanofabrication or chemical treatment. For commercial applications microwell plates are fabricated either by injection molding or vacuum forming;[33] however, we are mindful that the surface roughness of the pillars may be challenging to replicate with these techniques. This would ultimately depend on the mold resolution, but even if the pillars exhibited a sharp edge, they may be subjected to a finishing method including, but not limited to, sanding or scrubbing. For mass production of pillar plates, these and other fabrication methods warrant further investigation.

Overall, we have developed and characterized a novel platform to carry out colorimetric assays on suspended droplets. Although limited to these type of assays, our platform shows potential to be expanded to other types of assays, such as fluorometric or chemiluminescent assays, provided an appropriate detector is employed. Evaporation, far from being undesirable feature of microtiter plates, can be exploited to preconcentrate samples and also act as a natural mixing strategy. We anticipate that plate readers could be used to scan the pillar platform, but have yet to determine the optimal models and conditions under which results comparable to those from our custom system in terms of limit of detection and dynamic range can be obtained. In addition, our platform could be interfaced with microplate robotic systems or simply used with a pipet. Future studies will focus on expanding this method to other bioassays such as enzyme-linked immunosorbent assay (ELISA). When combined with smartphone cameras, the pillar assay may become an alternative low-cost platform for diagnostics.

ASSOCIATED CONTENT

Supporting Information

The Supporting Information is available free of charge on the ACS Publications website at DOI: 10.1021/acs.analchem.6b01657.

DOI: 10.1021/acs.analchem.6b01657
Anal. Chem. 2016, 88, 7312−7317

Video 1, visualization of Marangoni flow in a droplet containing fluorescent microparticles (MPG)
Video 2, visualization of Marangoni flow in a glucose colorimetric assay in a droplet (MPG)

AUTHOR INFORMATION

Corresponding Author

*E-mail: jlgarciac@cinvestav.mx.

Author Contributions

The manuscript was written through contributions of all authors. All authors have given approval to the final version of the manuscript.

Notes

The authors declare no competing financial interest.

ACKNOWLEDGMENTS

This work was funded by Fundación Miguel Alemán and CONACYT, Grant Nos. 256097 and 262771.

REFERENCES

(1) Banks, P. *Drug Discovery World* **2009**, *Spring*, 85−90.
(2) Burbaum, J. J. *Drug Discovery Today* **1998**, *3*, 313−322.
(3) Mayr, L. M.; Fuerst, P. *J. Biomol. Screening* **2008**, *13*, 443−448.
(4) Tan, H. Y.; Ng, T. W.; Neild, A.; Liew, O. W. *J. Biomol. Screening* **2010**, *15*, 1160−1164.
(5) Mayer, G.; Schober, A.; Kohler, J. M. *Rev. Mol. Biotechnol.* **2001**, *82*, 137−159.
(6) Lye, J. K.; Ng, T. W.; Neild, A.; Liew, O. W. *Anal. Biochem.* **2011**, *410*, 152−154.
(7) Mitre, E.; Schulze, M.; Cumme, G. A.; Rossler, F.; Rausch, T.; Rhode, H. *J. Biomol. Screening* **2007**, *12*, 361−369.
(8) De Angelis, F.; Gentile, F.; Mecarini, F.; Das, G.; Moretti, M.; Candeloro, P.; Coluccio, M. L.; Cojoc, G.; Accardo, A.; Liberale, C.; Zaccaria, R. P.; Perozziello, G.; Tirinato, L.; Toma, A.; Cuda, G.; Cingolani, R.; Di Fabrizio, E. *Nat. Photonics* **2011**, *5*, 682−687.
(9) McLane, J.; Wu, C.; Khine, M. *Adv. Mater. Interfaces* **2015**, *2*, 1400034.
(10) Choi, C. H.; Kim, C. J. *Langmuir* **2009**, *25*, 7561−7567.
(11) Barmi, M. R.; Meinhart, C. D. *J. Phys. Chem. B* **2014**, *118*, 2414−2421.
(12) Trantum, J. R.; Baglia, M. L.; Eagleton, Z. E.; Mernaugh, R. L.; Haselton, F. R. *Lab Chip* **2014**, *14*, 315−324.
(13) Barash, L. Y.; Bigioni, T. P.; Vinokur, V. M.; Shchur, L. N. *Phys. Rev. E* **2009**, *79*, 046301.
(14) Hu, H.; Larson, R. G. *J. Phys. Chem. B* **2006**, *110*, 7090−7094.
(15) Deegan, R. D. *Phys. Rev. E: Stat. Phys., Plasmas, Fluids, Relat. Interdiscip. Top.* **2000**, *61*, 475−485.
(16) Trantum, J. R.; Eagleton, Z. E.; Patil, C. A.; Tucker-Schwartz, J. M.; Baglia, M. L.; Skala, M. C.; Haselton, F. R. *Langmuir* **2013**, *29*, 6221−6231.
(17) Ristenpart, W. D.; Kim, P. G.; Domingues, C.; Wan, J.; Stone, H. A. *Phys. Rev. Lett.* **2007**, *99*, 234502.
(18) Wong, T. S.; Chen, T. H.; Shen, X. Y.; Ho, C. M. *Anal. Chem.* **2011**, *83*, 1871−1873.
(19) Trantum, J. R.; Wright, D. W.; Haselton, F. R. *Langmuir* **2012**, *28*, 2187−2193.
(20) Gulka, C. P.; Swartz, J. D.; Trantum, J. R.; Davis, K. M.; Peak, C. M.; Denton, A. J.; Haselton, F. R.; Wright, D. W. *ACS Appl. Mater. Interfaces* **2014**, *6*, 6257−6263.
(21) Larson, R. G. *Angew. Chem., Int. Ed.* **2012**, *51*, 2546−2548.
(22) Hu, H.; Larson, R. G. *Langmuir* **2005**, *21*, 3972−3980.
(23) Oliveira, K. A.; Medrado e Silva, P. B.; de Souza, F. R.; Martins, F. T.; Coltro, W. K. T. *Anal. Methods* **2014**, *6*, 4995−5000.
(24) Wang, C.; Sheng, Z. H.; Ouyang, J.; Xu, J. J.; Chen, H. Y.; Xia, X. H. *ChemPhysChem* **2012**, *13*, 762−768.
(25) Martinez, A. W.; Phillips, S. T.; Butte, M. J.; Whitesides, G. M. *Angew. Chem., Int. Ed.* **2007**, *46*, 1318−1320.
(26) Martinez, A. W.; Phillips, S. T.; Carrilho, E.; Thomas, S. W.; Sindi, H.; Whitesides, G. M. *Anal. Chem.* **2008**, *80*, 3699−3707.
(27) Dak, P.; Ebrahimi, A.; Alam, M. A. *Lab Chip* **2014**, *14*, 2469−2479.
(28) Ebrahimi, A.; Dak, P.; Salm, E.; Dash, S.; Garimella, S. V.; Bashir, R.; Alam, M. A. *Lab Chip* **2013**, *13*, 4248−4256.
(29) Shao, F. F.; Ng, T. W.; Liew, O. W.; Fu, J.; Sridhar, T. *Soft Matter* **2012**, *8*, 3563−3569.
(30) Hashimoto, M.; Sakamoto, N.; Upadhyay, S.; Fukuda, J.; Suzuki, H. *Biosens. Bioelectron.* **2007**, *22*, 3154−3160.
(31) Yanagimachi, I.; Nashida, N.; Iwasa, K.; Suzuki, H. *IEEJ Trans. Electr. Electron. Eng.* **2009**, *4*, 365−371.
(32) Gentile, F.; Coluccio, M. L.; Coppede, N.; Mecarini, F.; Das, G.; Liberale, C.; Tirinato, L.; Leoncini, M.; Perozziello, G.; Candeloro, P.; De Angelis, F.; Di Fabrizio, E. *ACS Appl. Mater. Interfaces* **2012**, *4*, 3213−3224.
(33) Mikkelsen, S. R.; Corton, E. *Bioanalytical Chemistry*, 2nd ed.; John Wiley & Sons: Hoboken, NJ, 2016; p 463.

DOI: 10.1021/acs.analchem.6b01657
Anal. Chem. 2016, 88, 7312−7317